Article

Experiment and Calculation of Solid−Liquid Phase Equilibria in the Ternary System SrCl$_2$−SrBr$_2$−H$_2$O at T = 273, 298, and 323 K

Xue-Ping Zhang, Han-Zhong Zhang, Lan-Rong Zhao, and Shi-Hua Sang*

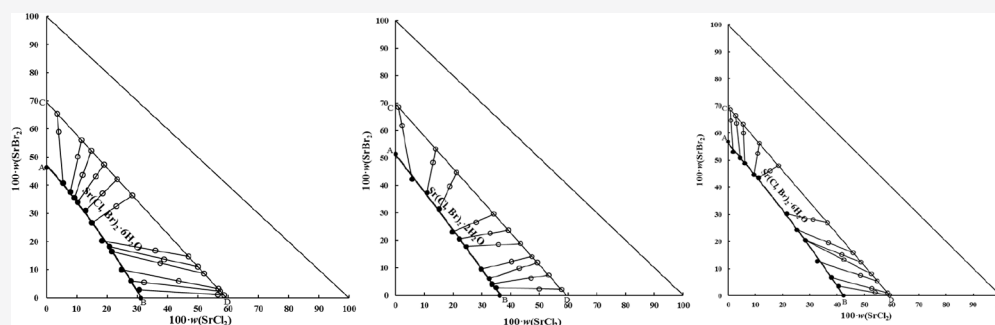Cite This: https://dx.doi.org/10.1021/acs.jced.0c00478

Read Online

ACCESS | ▥ Metrics & More | ▤ Article Recommendations

ABSTRACT: This work describes the solid−liquid phase equilibria in the ternary system SrCl$_2$−SrBr$_2$−H$_2$O at T = 273, 298, and 323 K based on the method of isothermal dissolution equilibrium. Since saturated liquid phases and humid residue compositions for a series of synthetic brines were determined simultaneously, the measured equilibrium tie lines were constructed. At the same time, the corresponding equilibrium solid phases were identified by using the Schreinemakers' method supplemented with X-ray powder diffraction. The experimental phase diagrams of the system SrCl$_2$−SrBr$_2$−H$_2$O at T = 273, 298, and 323 K were established according to the theory of phase diagram for water salt system. It is found that the type of the system is classified as completely solid solution type due to formation of solid solution Sr(Cl, Br)$_2$·6H$_2$O. The phase diagrams of the ternary system SrCl$_2$−SrBr$_2$−H$_2$O at 273, 298, and 323 K are constituted of one univariant solubility curve and one solid crystalline phase region corresponding to Sr(Cl, Br)$_2$·6H$_2$O, without any invariant point. The Pitzer equation was selected to calculate the solubility data in the ternary system SrCl$_2$−SrBr$_2$−H$_2$O at T = 273, 298, and 323 K. The solubility modeling approach achieved good agreement with experimental solubility data.

1. INTRODUCTION

The underground brines in the Sichuan Basin are widely distributed and reserve abundantly. In addition to sodium chloride, various available metal ions such as K$^+$, Br$^−$, I$^−$, B^{3+}, Li$^+$, Sr^{2+}, and Rb$^+$, etc., are rich in brines, and their contents exceed the minimum industrial grade of comprehensive utilization, which constitute a superior liquid mineral in Sichuan Basin. Consequently, conducting research on the phase equilibrium of complex multicomponent systems is essential for the utilization of liquid minerals in the region. Strontium ore is found in nature as the liquid brines or solid minerals celestite (SrSO$_4$) and strontianite (SrCO$_3$). Strontium compounds are applied to generating various products in the fields of chemical engineering, electronics, aerospace, and medicine, etc.[1] Acting as a subsystem in a complex multicomponent system, the ternary system SrCl$_2$−SrBr$_2$−H$_2$O is a focus for conducting multiple temperature phase equilibrium research and is of practical significance for obtaining valuable strontium compounds.

Investigations on the phase diagram of a strontium-containing water−salt system are mainly focused on strontium chloride,

and the phase equilibrium studies of strontium bromide are relatively scarce. In the phase equilibrium study of the ternary system concerning SrCl$_2$, the solubility of MgCl$_2$−SrCl$_2$−H$_2$O in the range of 18−100 °C and CaCl$_2$−SrCl$_2$−H$_2$O in the temperature range from 18 to 114 °C have been measured entirely.[2,3] A multitemperature study was also conducted on the SrCl$_2$−H$_2$O system in the temperature range of 18−114 °C, and it was found that the dehydration conversion temperature of strontium chloride hexahydrate to strontium chloride dihydrate is 61.3 °C.[4] Moreover, aiming at the utilization of strontium-rich underground brine in the Sichuan Basin, research on phase equilibrium of ternary systems NaCl−SrCl$_2$−H$_2$O and KCl−SrCl$_2$−H$_2$O at 348 K was carried out.[5] Regarding the phase

diagram of water−salt containing strontium bromide, the ternary subsystem mainly includes $MgBr_2$−$SrBr_2$−H_2O at 298 and 323 K,[6] and $NaBr$−$SrBr_2$−H_2O and KBr−$SrBr_2$−H_2O at 288, 308, and 323 K.[7−9] The phase equilibrium in quaternary system $NaBr$−KBr−$SrBr_2$−H_2O at 348 K was investigated, which indicated that strontium bromide hexahydrate can be widely present at a temperature within 348 K.[10]

It is generally acknowledged that solid solutions can be formed in a solid−liquid mixture in which chloride and bromine coexist. The so-called solid solution means that a small number of two salts having one common ion form a uniform mixed crystal of atoms, ions, or molecules dispersed in a solid form, that is, one or several solid phases having a variable composition.[11] Although there is a wide investigation concerning ternary systems $NaCl$−$NaBr$−H_2O, KCl−KBr−H_2O, and $MgCl_2$−$MgBr_2$−H_2O over a wide temperature range[12−19] and $CaCl_2$−$CaBr_2$−H_2O and $LiCl$−$LiBr$−H_2O at 288 K,[20] the ternary system $SrCl_2$−$SrBr_2$−H_2O has not been conducted at any temperature in the literature.

The research task of this work is to investigate the stable solid−liquid equilibrium of the ternary system $SrCl_2$−$SrBr_2$−H_2O at 273, 298, and 323 K and simulate the calculation solubility on the basis of the Pitzer equation. On the basis of the completion of phase equilibrium experiments and solubility simulation calculations on this system at 273, 298, and 323 K, the dissolution and interaction mechanisms between the components have been further explored. The results offer basic thermodynamic data in exploiting compounds containing strontium and lay a theoretical foundation for further elucidating the formation of brine.

2. EXPERIMENTS

2.1. Reagents and Instruments. The sample description table is noted with Table 1, in which the chemical regents, mass

Table 1. Sample Description Table

chemical reagent	CAS Reg. No.	mass fraction purity/%	supplier	analysis method
$SrCl_2·6H_2O$	10025-70-4	≥99.5	Chengdu Kelong Chemical Reagent Manufacture, China	silver nitrate volumetric method
$SrBr_2·6H_2O$	10476-81-0	≥99.0	Chengdu Kelong Chemical Reagent Manufacture, China	silver nitrate volumetric method

fraction purity, supplier, and analysis method are listed. An electronic analytical balance of OHAUS AR2140 type with a maximum capacity of 210 g and a readability of 0.0001 g was supplied by Shenzhen Yihuaxin Electronics Co., Ltd. The high purity water with at least a resistivity of 18 MΩ·cm was prepared by ultrapure water instrument of UPT-11-40L type. A DHJF-4002 type low temperature, constant temperature stirring reaction bath with a temperature range from 233 to 372 K and a stability of 0.2° supplied by the Zhengzhou Greatwall Scientific Industrial and Tread Co., Ltd. was involved in accelerating the dissolution equilibrium of the samples and maintaining the temperature at 273, 298, and 323 K, respectively. An electric thermal blowing drybox (101-2AB, supplied by the Tianjin Taisite Instrument Co., Ltd.) was employed to dry the solid samples.

2.2. Experimental Method. The solubility of each component in the ternary system at the experimental temperature was measured by the isothermal dissolution equilibrium

method. The isothermal solid−liquid phase equilibrium experiments were carried out in accordance with the following steps. First, in the 250 mL grinding round-bottom flask, a certain proportion of the solid raw material was mixed with the moderate amount of ultrapure water. In addition, the above step was carried out in the constant temperature stirring reaction bath. The presence of solid throughout the dissolution equilibrium process must be ensured, which is for the sake of the production of a saturated solution. The samples were dissolved in water for 24, 48, and 72 h at the acceleration of magnetic stirring controlling the temperature at 323, 298, and 273 K, respectively. After the exhaustive mixing is completed, the magnetic mixer was switched off. The clarified supernatant liquor was acquired with the condition of a solid−liquid mixture left for 24 h and obvious stratification. When the dissolution rate of each salt is equal to the crystallization rate, the solid phase and the liquid phase are considered to reach a phase equilibrium state. The supernatant at the invariant point was periodically taken for chemical analysis. The constant solubility of each salt was taken as a sign of achieving solid−liquid stable phase equilibrium. After equilibration, the supernatant was removed by a quick pipet and diluted to determine the concentration, so that the solubility of each substance in the saturated solution was calculated. The Schreinemakers method[21] combined with XRD was used to identify the crystalline solid phase composition corresponding to the saturated liquid phase at the dissolution equilibrium.

2.3. Analytical Methods.[22] The total content of chloride ion and bromine ion was determined by using silver nitrate volumetric method with a potassium chromate solution as the indicator (uncertainty of 0.3 mass %). The concentration of bromine ion was determined by the method of sodium hypochlorite iodometry (uncertainty of 0.5 mass %). The measurement principle is as follows. In the brine of pH 5−7, the hypochlorite ionized by the bromide ion is oxidized to the bromate ion, and then the excess hypochlorite is neutralized by sodium formate. Finally, the bromide ion content can be determined by measuring the generated bromate ion by iodometric method. The content of each equilibrium sample was evaluated on the basis of the average of three determination results.

3. RESULTS AND DISCUSSION

3.1. Binary Systems $SrBr_2$−H_2O and $SrCl_2$−H_2O at 273, 298, and 323 K and 0.1 MPa. The solubility for the binary systems $SrBr_2$−H_2O and $SrCl_2$−H_2O at T = 273, 298, and 323 K were determined in multiple available studies, which were plotted in Figure 1. The solubility of $SrBr_2$ in the binary system $SrBr_2$−H_2O at 273, 298, and 323 K with the values 46.39%, 51.52%, and 56.80%, respectively, are in good agreement with the reported values 46.00%, 51.70%, and 57.60% in the *CRC Handbook of Chemistry and Physics*.[23] The calculated relative standard deviations at 273, 298, and 323 K are 0.85%, 0.35%, and 1.39%, respectively. For another binary system $SrCl_2$−H_2O, the solubility data of $SrCl_2$ are 31.08% (T = 273 K), 36.19% (T = 298 K), and 42.39% (T = 323 K), which are similar to the former experimental data 31.94% (T = 273 K), 35.37% (T = 298 K), and 41.94% (T = 323 K) according to the CRC handbook,[23] with the relative standard deviations 2.57%, 2.32%, and 1.07% at 273, 298, and 323 K, respectively. The experimental measurement deviation of solubility is within a certain allowable range, which shows that the experimental process and measurement results are reliable.
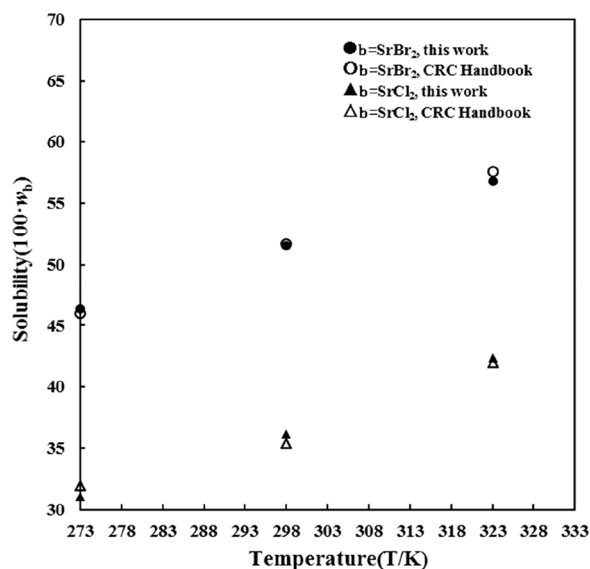
Figure 1. Comparison of solubility for salt b (b = $SrBr_2$ and $SrCl_2$) at T = 273, 298, and 323 K: ● (b = $SrBr_2$), this work; ○ (b = $SrBr_2$), data from ref 23; ▲ (b = $SrCl_2$), this work; △ (b = $SrCl_2$), data from ref 23.

3.2. Ternary System $SrCl_2$−$SrBr_2$−H_2O at 273, 298, and 323 K and 0.1 MPa. The experimental solubilities in the ternary system $SrCl_2$−$SrBr_2$−H_2O at 273, 298, and 323 K and 0.1 MPa are listed in Table 2. The concentration of the solution or wet solid for the mineral b is represented by $100w(b)$, in which the symbol w is the mass percentage of salt in the system. On the basis of the composition of the saturated liquid phase, wet solid phase, and solid phase, the isothermal phase diagrams at T = 273, 298, and 323 K were constructed, as shown in Figures 2, 3, and 4, respectively. The mass fractions $100w(SrCl_2)$ and $100w(SrBr_2)$ were expressed as X axis and Y axis in phase diagrams, respectively.

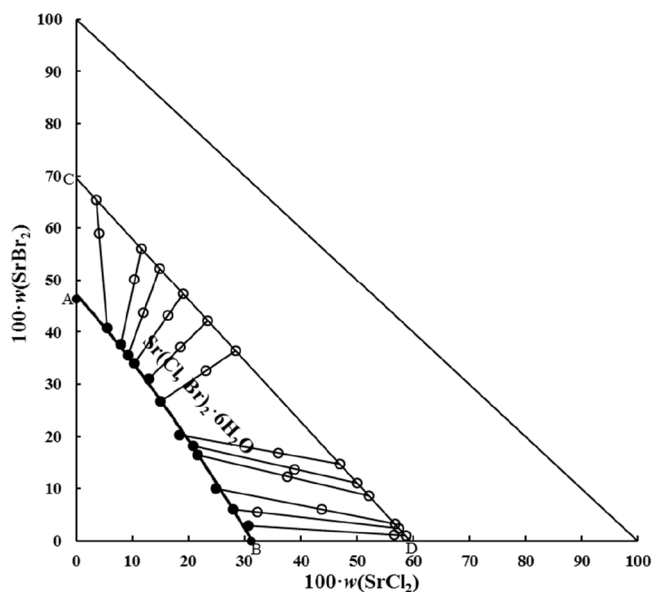**Figure 2.** Solubility diagram of the ternary system $SrCl_2$−$SrBr_2$−H_2O at 273 K and 0.1 MPa: ●, saturated liquid composition point; ○, wet solid phase composition point; tie line, solubility line; dotted line, wet slag line.

Figure 3. Solubility diagram of the ternary system $SrCl_2$−$SrBr_2$−H_2O at 298 K and 0.1 MPa: ●, saturated liquid composition point; ○, wet solid phase composition point; tie line, solubility line; dotted line, wet slag line.

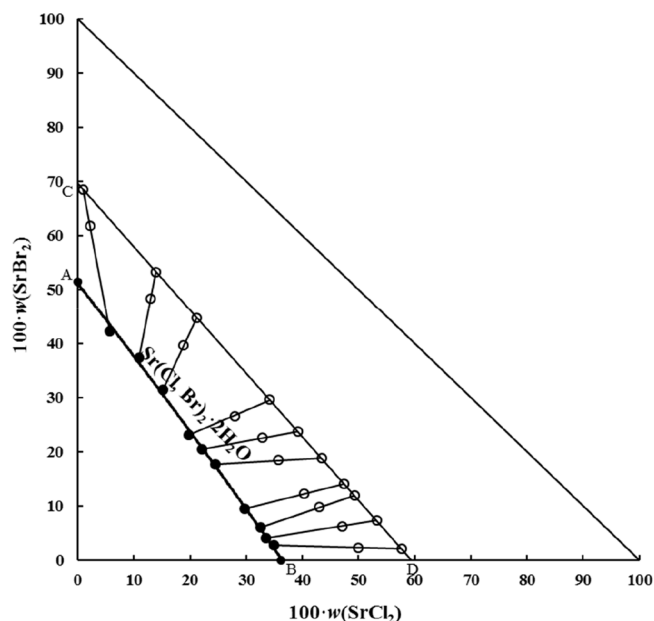**Figure 4.** Solubility diagram of the ternary system $SrCl_2$−$SrBr_2$−H_2O at 323 K and 0.1 MPa: ●, saturated liquid composition point; ○, wet solid phase composition point; tie line, solubility line; dotted line, wet slag line.

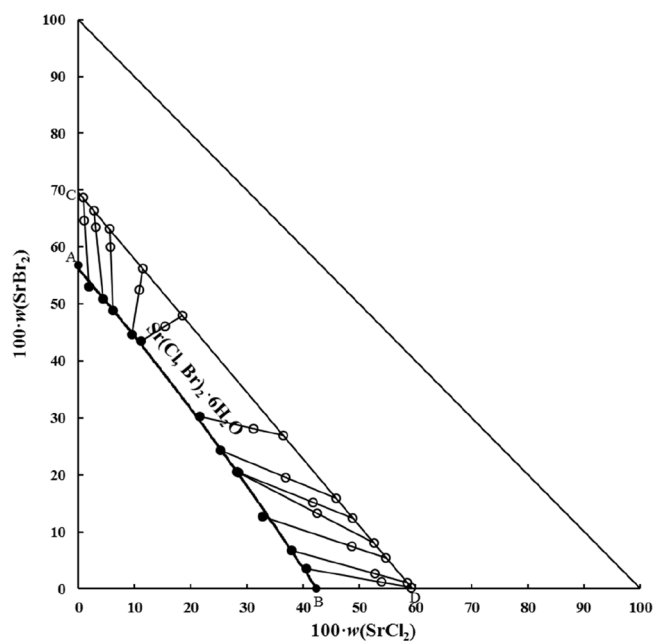The Table 2 and corresponding phase diagrams Figures 2, 3, and 4 reveal that isothermal solubility diagrams of the ternary $SrCl_2$−$SrBr_2$−H_2O at 273, 298, and 323 K are classified as thoroughly miscible solid solution phase diagrams. Points A, B, C, and D stand for invariant point in binary system $SrBr_2$−H_2O, invariant point in binary system $SrCl_2$−H_2O, single solid phase point for $SrBr_2$·$6H_2O$, and single solid phase point for $SrCl_2$·$6H_2O$ in the phase diagrams, respectively. The phase diagrams are divided into two regions by one univariant curve noted as AB curve. There is only a crystalline region of solid solution Sr(Cl,

Table 2. Solubilities in the Ternary System SrCl$_2$–SrBr$_2$–H$_2$O at 273, 298, and 323 K and 0.1 MPa[a]

T/K	no.	composn of soln (100w(b))		composn of wet solid (100w(b))		composn of solid soln (100w(b))		solid phase
		b = SrCl$_2$	b = SrBr$_2$	b = SrCl$_2$	b = SrBr$_2$	b = SrCl$_2$	b = SrBr$_2$	
273	1,A	0.00	46.39					SrBr$_2$·6H$_2$O
	2	5.47	40.83	4.11	58.93	3.63	65.35	Sr(Cl$_{0.0798}$, Br$_{0.9202}$)$_2$·6H$_2$O
	3	7.93	37.57	10.44	50.12	11.62	56.00	Sr(Cl$_{0.2446}$, Br$_{0.7554}$)$_2$·6H$_2$O
	4	9.21	35.49	12.00	43.67	14.90	52.16	Sr(Cl$_{0.3084}$, Br$_{0.6916}$)$_2$·6H$_2$O
	5	10.37	33.98	16.26	43.13	18.99	47.37	Sr(Cl$_{0.3849}$, Br$_{0.6151}$)$_2$·6H$_2$O
	6	12.97	31.06	18.56	37.05	23.39	42.22	Sr(Cl$_{0.4637}$, Br$_{0.5363}$)$_2$·6H$_2$O
	7	15.10	26.66	23.16	32.53	28.41	36.35	Sr(Cl$_{0.5495}$, Br$_{0.4505}$)$_2$·6H$_2$O
	8	18.48	20.24	36.00	16.82	46.91	14.69	Sr(Cl$_{0.8329}$, Br$_{0.1671}$)$_2$·6H$_2$O
	9	20.80	18.18	38.87	13.74	50.07	10.99	Sr(Cl$_{0.8767}$, Br$_{0.1233}$)$_2$·6H$_2$O
	10	21.71	16.43	37.58	12.36	52.08	8.46	Sr(Cl$_{0.9039}$, Br$_{0.0961}$)$_2$·6H$_2$O
	11	24.91	9.98	43.68	5.98	56.73	3.20	Sr(Cl$_{0.9651}$, Br$_{0.0349}$)$_2$·6H$_2$O
	12	27.97	5.97	32.23	5.46	57.37	2.45	Sr(Cl$_{0.9734}$, Br$_{0.0266}$)$_2$·6H$_2$O
	13	30.59	2.82	56.58	1.09	58.65	0.95	Sr(Cl$_{0.9897}$, Br$_{0.0103}$)$_2$·6H$_2$O
	14,B	31.08	0.00					SrCl$_2$·6H$_2$O
298	1,A	0.00	51.42					SrBr$_2$·6H$_2$O
	2	5.74	42.32	2.18	61.73	0.94	68.50	Sr(Cl$_{0.0210}$, Br$_{0.9790}$)$_2$·6H$_2$O
	3	10.90	37.31	12.99	48.29	13.94	53.28	Sr(Cl$_{0.2900}$, Br$_{0.7100}$)$_2$·6H$_2$O
	4	15.15	31.42	18.86	39.60	21.21	44.78	Sr(Cl$_{0.4250}$, Br$_{0.5750}$)$_2$·6H$_2$O
	5	19.74	23.16	28.02	26.52	34.18	29.59	Sr(Cl$_{0.6432}$, Br$_{0.3568}$)$_2$·6H$_2$O
	6	22.09	20.44	32.86	22.58	39.11	23.82	Sr(Cl$_{0.7193}$, Br$_{0.2807}$)$_2$·6H$_2$O
	7	24.50	17.61	35.71	18.49	43.40	17.61	Sr(Cl$_{0.7937}$, Br$_{0.2063}$)$_2$·6H$_2$O
	8	29.71	9.52	40.29	12.23	47.45	14.06	Sr(Cl$_{0.8404}$, Br$_{0.1596}$)$_2$·6H$_2$O
	9	32.50	6.07	42.93	9.73	49.25	11.95	Sr(Cl$_{0.8655}$, Br$_{0.1345}$)$_2$·6H$_2$O
	10	33.56	4.02	47.14	6.27	53.24	7.28	Sr(Cl$_{0.9194}$, Br$_{0.0806}$)$_2$·6H$_2$O
	11	34.86	2.74	49.92	2.27	57.73	2.03	Sr(Cl$_{0.9780}$, Br$_{0.0220}$)$_2$·6H$_2$O
	12,B	36.19	0.00					SrCl$_2$·6H$_2$O
323	1,A	0.00	56.80					SrBr$_2$·6H$_2$O
	2	1.81	53.09	1.04	64.66	0.77	68.70	Sr(Cl$_{0.0172}$, Br$_{0.9828}$)$_2$·6H$_2$O
	3	4.42	50.89	3.03	63.51	2.71	66.43	Sr(Cl$_{0.0599}$, Br$_{0.9401}$)$_2$·6H$_2$O
	4	6.18	48.91	5.63	60.04	5.47	63.19	Sr(Cl$_{0.1190}$, Br$_{0.8810}$)$_2$·6H$_2$O
	5	9.52	44.57	10.78	52.52	11.38	56.28	Sr(Cl$_{0.2399}$, Br$_{0.7601}$)$_2$·6H$_2$O
	6	11.13	43.47	15.37	46.12	18.43	48.03	Sr(Cl$_{0.3746}$, Br$_{0.6254}$)$_2$·6H$_2$O
	7	21.55	30.28	31.13	28.11	36.48	26.90	Sr(Cl$_{0.6791}$, Br$_{0.3209}$)$_2$·6H$_2$O
	8	25.31	24.27	36.89	19.57	45.85	15.93	Sr(Cl$_{0.8179}$, Br$_{0.1821}$)$_2$·6H$_2$O
	9	28.13	20.57	41.74	15.20	48.88	12.38	Sr(Cl$_{0.8604}$, Br$_{0.1396}$)$_2$·6H$_2$O
	10	28.51	20.43	42.52	13.22	52.59	8.04	Sr(Cl$_{0.9108}$, Br$_{0.0892}$)$_2$·6H$_2$O
	11	32.79	12.71	48.61	7.44	54.75	5.39	Sr(Cl$_{0.9407}$, Br$_{0.0593}$)$_2$·6H$_2$O
	12	37.86	6.81	52.76	2.69	58.52	1.10	Sr(Cl$_{0.9881}$, Br$_{0.0119}$)$_2$·6H$_2$O
	13	40.53	3.49	54.01	1.16	59.26	0.26	Sr(Cl$_{0.9972}$, Br$_{0.0028}$)$_2$·6H$_2$O
	14,B	42.39	0.00					SrCl$_2$·6H$_2$O

[a]Notation: Standard uncertainties for temperature and pressure are $u(T)$ = 0.1 K and $u(P)$ = 1 kPa, respectively. Relative standard uncertainties for solubility are $u_r(w(SrCl_2))$ = 0.005 and $u_r(w(SrBr_2))$ = 0.005.

Br)$_2$·6H$_2$O formed between SrCl$_2$·6H$_2$O and SrBr$_2$·6H$_2$O in the phase diagrams. Under the dissolution curve AB of the solid solution, an unsaturated liquid phase region occupies the entire space. The composition of the solid phase occurs as a continuous transition from pure salt SrBr$_2$·6H$_2$O to another pure salt SrCl$_2$·6H$_2$O at the solid phase boundary line CD. It can be found by comparing the phase diagrams at three temperatures that the complete solid solution is formed over a wide temperature range. As the temperature changes between 273 and 323 K, the crystalline form of the solid solution does not change, and it contains six molecules of crystalline water consistent with the single salt. Furthermore, it is obviously with inspection that the crystallization region of the solid solution gradually decreases with increasing temperature owing to the positive correlation between the solubility of SrCl$_2$ and SrBr$_2$ with temperature.

The separated wet residue was washed with absolute ethanol and then dried at the experimental temperature to remove the adsorbed water on the surface. The results of chemical analysis showed that the solid solution molecule contained six crystal water molecules in the temperature range of 273–323 K. The X-ray powder crystal diffraction patterns of the solid solution Sr(Cl, Br)$_2$·6H$_2$O at 273, 298, and 323 K were depicted in Figures 5, 6, and 7, respectively. Due to the absence of a standard card for solid solution Sr(Cl, Br)$_2$·6H$_2$O, the reference spectra of SrCl$_2$·6H$_2$O (PDF No. 06-0073) and SrBr$_2$·6H$_2$O (PDF No. 060176) were selected to reflect the generated solid solution. The results reveal that the position of the diffraction peak for the solid solution Sr(Cl, Br)$_2$·6H$_2$O is between SrBr$_2$·6H$_2$O and
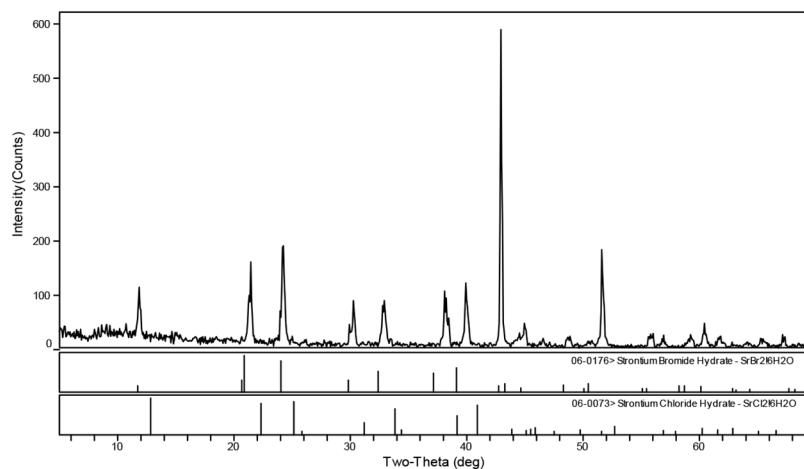
Figure 5. X-ray powder crystal diffraction pattern of the solid solution $Sr(Cl_{0.5495}, Br_{0.4505})_2 \cdot 6H_2O$ (point 7) in the ternary system $SrCl_2-SrBr_2-H_2O$ at 273 K and 0.1 MPa.

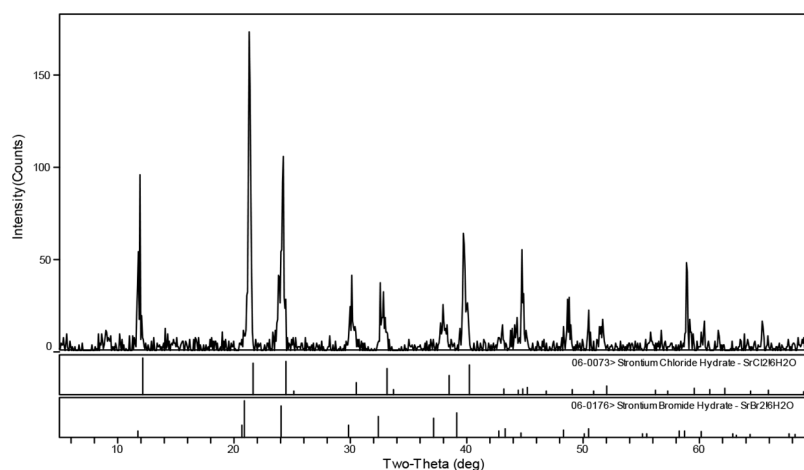**Figure 6.** X-ray powder crystal diffraction pattern of the solid solution $Sr(Cl_{0.6432}, Br_{0.3568})_2 \cdot 6H_2O$ (point 5) in the ternary system $SrCl_2-SrBr_2-H_2O$ at 298 K and 0.1 MPa.
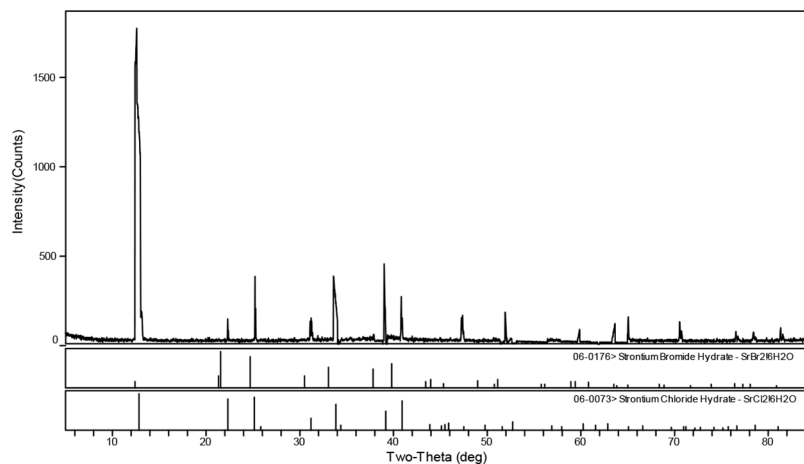
Figure 7. X-ray powder crystal diffraction pattern of solid solution $Sr(Cl_{0.6791}, Br_{0.3209})_2 \cdot 6H_2O$ (point 7) in the ternary system $SrCl_2-SrBr_2-H_2O$ at 323 K and 0.1 MPa.

$SrCl_2 \cdot 6H_2O$ at 273, 298, and 323 K, which further validate the solid phase identification on the basis of the Schreinemakers method. Judging from the characteristics of the entire phase diagram, there is no invariant point and the equilibrium connecting line is divergent, which also shows that the phase diagram belongs to the solid solution type.

3.3. Prediction of Solubility. Electrolyte solution is largely located in the fields of chemical engineering, geochemistry, soil science, and hydrometallurgy. As a matter of fact, various

E

theoretical research models are available for electrolyte solution, among which Pitzer electrolyte solution theoretical model equation is widely used because of its simple form and compact structure, and being applied to practical high concentration solutions.[24−26] The calculation formula of permeability coefficient and activity coefficient derived from Pitzer theory can be used to simulate the solubility with a view to salt in a multicomponent water−salt system, to calculate the reaction ratio of materials in chemical processes, and to perform a series of calculations for isothermal evaporation of brine. Relevant studies have proved that Pitzer's basic equation is reliable.[27,28] The detailed Pitzer equation is available in refs 25 and 29. The basic equations are shown as follows:

$$
\phi - 1 = \left(\sum_i m_i\right)^{-1} \left\{ 2\left[-A^\phi I^{3/2}/(1 + 1.2I^{1/2}) \right.\right.
$$

$$
+ \sum_{c=1}^{N_c}\sum_{a=1}^{N_a} m_c m_a (B_{ca}^\phi + Z C_{ca})
$$

$$
+ \sum_{c=1}^{N_c-1}\sum_{c'=c+1}^{N_c} m_c m_{c'}\left(\Phi_{cc'}^\Phi + \sum_{a=1}^{N_a} m_a \psi_{cc'a}\right)
$$

$$
+ \sum_{c=1}^{N_c-1}\sum_{c'=c+1}^{N_c} m_c m_{c'}\left(\Phi_{cc'}^\Phi + \sum_{a=1}^{N_a} m_a \psi_{cc'a}\right)
$$

$$
\left.\left.+ \sum_{a=1}^{N_a-1}\sum_{a'=a+1}^{N_a} m_a m_{a'}\left(\Phi_{aa'}^\Phi + \sum_{c=1}^{N_c} m_c \psi_{aa'c}\right)\right]\right\} \tag{1}
$$

$$
\ln \gamma_M = Z_M^2 F + \sum_{a=1}^{N_a} m_a (2B_{Ma} + Z C_{Ma})
$$

$$
+ \sum_{c=1}^{N_c} m_c \left(2\Phi_{Mc} + \sum_{a=1}^{N_a} m_a \psi_{Mca}\right)
$$

$$
+ \sum_{a=1}^{N_a-1}\sum_{a'=a+1}^{N_a} m_a m_{a'} \psi_{aa'M} + |Z_M| \sum_{c=1}^{N_c}\sum_{a=1}^{N_a} m_c m_a C_{ca} \tag{2}
$$

$$
\ln \gamma_X = Z_X^2 F + \sum_{c=1}^{N_c} m_c (2B_{cX} + Z C_{cX})
$$

$$
+ \sum_{a=1}^{N_a} m_a \left(2\Phi_{Xa} + \sum_{c=1}^{N_c} m_c \psi_{Xac}\right)
$$

$$
+ \sum_{c=1}^{N_c-1}\sum_{c'=c+1}^{N_c} m_c m_{c'} \psi_{cc'M} + |Z_X| \sum_{c=1}^{N_c}\sum_{a=1}^{N_a} m_c m_a C_{ca} \tag{3}
$$

In eqs 1, 2, and 3, where ϕ and γ_i denote osmotic coefficient and activity coefficient; M, c, and c' represent cations. Similarly, X, a, and a' represent anions. The symbols Z_i and m_i express the valence and molality (mol·kg^{-1}) of the ion, respectively. The marks N_c and N_a represent the number of cations and anions, respectively.

The Pitzer single-salt parameters β^0, β^1, and C^ϕ for SrCl$_2$ and SrBr$_2$ at 273, 298, and 323 K listed in Table 3 were calculated using chemical models given by literature, which were used in predicting the solubility isotherm.[30,31] On the basis of evaluated activity and osmotic coefficients for SrCl$_2$ and SrBr$_2$ in aqueous

Table 3. Values of Pitzer Single-Salt Parameters

salt	temp/K	β^0	β^1	C^ϕ	ref
SrCl$_2$·6H$_2$O	273	0.2652	1.5191	−0.005210	30
	298	0.2834	1.6256	−0.0003150	30
		0.2817	1.6167	−0.0007100	32
	323	0.2891	1.7091	−0.005880	30
		0.2122	6.3500	−0.02899	33
SrBr$_2$·6H$_2$O	273	0.3605	1.5212	−0.003718	31
	298	0.3311	1.7115	0.001200	31
		0.3241	1.7822	0.003440	32
	323	0.3017	1.9019	0.006118	31
		0.2115	6.3420	−0.03005	33

solutions, Pitzer single-salt parameters for them at 298 K were obtained and listed in Table 3.[32] By comparison with the previous available reference,[32] single-salt parameters (β^0, β^1, and C^ϕ) for SrCl$_2$ and SrBr$_2$ at 298 K[30,31] used in solubility simulation have similar values. In the early reported work, measured vapor pressures of aqueous solutions containing SrCl$_2$ or SrBr$_2$ have been used to calculate activity and osmotic coefficients.[33] By using the calculated activity coefficient data of SrCl$_2$ and SrBr$_2$ at 323 K, the single-salt parameters of them were fitted and listed in Table 3. The comparison indicated that an obvious numerical deviation was reflected in the single-salt parameter β^1 for SrCl$_2$ and SrBr$_2$ at 323 K. For the NaCl−NaBr−H$_2$O ternary system, isopiestic investigation was conducted in the literature.[34] And fitted two and three particles parameters were proved to be zero which is attributed to a fairly similar behavior of irons encountering water molecules.[35] Owing to the particularity of solid solution in the structure, the ions interaction mixing parameters $\theta_{Cl,Br}$ and $\Psi_{Sr,Cl,Br}$ in this system would be close to zero value. And two ion interaction mixing parameters $\theta_{Cl,Br}$ and $\Psi_{Sr,Cl,Br}$ were fitted in Table 4 by

Table 4. Values of Pitzer Mixing Ion-Interaction Parameters

temp/K	$\theta_{Cl,Br}$	$\psi_{Sr,Cl,Br}$
273	0.000138	0.001189
298	0.000356	0.000909
323	0.000482	0.000458
ref	this work	this work

solubility data of the ternary system SrCl$_2$−SrBr$_2$−H$_2$O using multiple linear regression method. In order to reflect the effect of temperature on the mixing parameters and to obtain the mixing parameters at any temperature in the study temperature range, the temperature independent equation applicable to the mixing parameters of the solid solution is established as a model by adjusting the constants selected in eq 4. The coefficients b_i ($i = 1$, 2, 3) in eq 4 for mixing parameters $\theta_{Cl,Br}$ and $\psi_{Sr,Cl,Br}$ of the ternary system SrCl$_2$−SrBr$_2$−H$_2$O were listed in Table 5.

$$
P(T) = b_1 + b_2 (T/K) + b_3 \ln(T/K) \tag{4}
$$

With regard to solid solution Sr(Cl$_X$, Br$_{1-X}$)$_2$·6H$_2$O, the solubility product constant (K_{sp}) can be expressed by eq 5, which is derived from the literature describing solubility prediction aiming at solid solution.[13,18,36,37] When K_{sp} is largely affected by variable solid phase composition, which is targeted at the solid solution system, the relationship between the equilibrium constant and the solid phase composition must be constructed. The functions shown in eqs 6 and 7 were obtained

Table 5. Coefficients b_i for Mixing Parameters $\theta_{Cl,Br}$ and $\psi_{Sr,Cl,Br}$ of the Ternary System $SrCl_2$–$SrBr_2$–H_2O

param	b_1	b_2	b_3	R^2	ref
$\theta_{Cl,Br}$ (273.15−323.15K)	−0.06193	-3.624×10^{-5}	0.01283	0.999	this work
$\psi_{Sr,Cl,Br}$ (273.15−323.15 K)	−0.1079	-9.561×10^{-5}	0.02409	0.999	this work

Table 6. Values of Regression Coefficients a_i for Solubility Equilibrium Constant ($\ln K_{sp}$) of Solid Solution $Sr(Cl_X, Br_{1-X})_2 \cdot 6H_2O$

temp/K	a_0	a_1	a_2	a_3	a_4	R^2	ref
273	5.9971	−5.9163	1.3075	3.8200	−2.4537	0.996	this work
298	6.9523	−7.6429	8.6405	−9.4783	6.0168	0.996	this work
323	8.0145	−12.8100	33.1130	−42.694	19.5870	0.997	this work

by polynomial fitting of the solid solution composition data. According to eqs 1−3, the mean activity coefficient ($\gamma_\pm$) and water activity can be expressed as eqs 8 and 9.

$$\ln K_{sp} = \ln(m_{Sr}\gamma_{Sr}) + 2X \ln(m_{Cl}\gamma_{Cl}) + 2(1 - X)$$

$$\ln(m_{Br}\gamma_{Br}) + 6 \ln a_w \qquad (5)$$

$$Y = a_0 + a_1X + a_2X^2 + a_3X^3 + a_4X^4 \qquad (6)$$

$$X = m_{Cl}/(m_{Cl} + m_{Br}) \qquad (7)$$

$$\gamma_\pm = (\gamma_{Sr}\gamma_{Cl}^2)^{1/3}, \qquad \gamma_\pm = (\gamma_{Sr}\gamma_{Br}^2)^{1/3} \qquad (8)$$

$$\ln a_w = -\phi(M_W/1000) \sum m_i \qquad (9)$$

In eq 6, solubility equilibrium constant ($\ln K_{sp}$) for solid solution was noted as Y. Regression coefficients fitted by multiple linear regression was represented by a_i ($i = 1, 2, 3, 4$). Mole fraction for $SrCl_2$ in solid solution was marked as X in eqs 5, 6, and 7. Coefficients a_i in eq 6 were listed in Table 6, in which a_0 was equal to the equilibrium constant ($\ln K_{sp}$) of $SrBr_2 \cdot 6H_2O$ with the value of 5.9971 ($T = 273$ K), 6.9523 ($T = 298$ K), and 8.0145 ($T = 323$ K), respectively. Using listed coefficients a_i in Table 6, the equilibrium constants ($\ln K_{sp}$) of $SrCl_2 \cdot 6H_2O$ were obtained as 2.7546 ($T = 273$ K), 4.4884 ($T = 298$ K), and 5.2105 ($T = 323$ K), respectively, and those values were confirmed as 3.4244 ($T = 273$ K), 4.3264 ($T = 298$ K), and 5.0172 ($T = 323$ K) in a reported reference.[38] On the basis of Pitzer single-salt parameters, mixing parameters, saturated solubility data, and mole fraction for $SrCl_2$ in solid solution, the solubility equilibrium constant ($\ln K_{sp}$) for solid solution $Sr(Cl_X, Br_{1-X})_2 \cdot 6H_2O$ was calculated. The obtained solubility equilibrium constants ($\ln K_{sp}$) of the $Sr(Cl, Br)_2 \cdot 6H_2O$ solid solution were presented graphically in Figure 8.

On the basis of the Pitzer equation for aqueous electrolyte solutions, the solubilities of the ternary system $SrCl_2$–$SrBr_2$–H_2O at 273, 298, and 323 K have been calculated using particle swarm optimization (PSO) algorithm. The comparison diagrams between experiment and calculation solubilities at 273, 298, and 323 K were given in Figures 9, 10, and 11. It also shows that the calculated values have a good agreement with the measured experimental data. The trend of the solubility curve obtained through model calculation and experimental measurement is roughly the same with a high degree of coincidence. These above results indicate that the Pitzer model can be applied to solid−liquid equilibrium calculations involving solid solution. The mean activity coefficients of strontium chloride and strontium bromide in the mixed equilibrium solution in the entire molality concentration range at 273, 298, and 323 K were also calculated, which were shown in Figures 12 and 13,
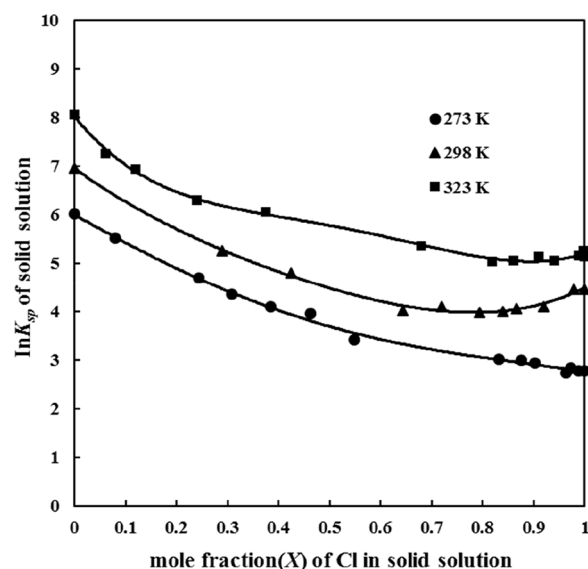
Figure 8. Solubility equilibrium constant ($\ln K_{sp}$) of solid solution versus mole fraction (X) of Cl in solid solution diagram at 273, 298, and 323 K
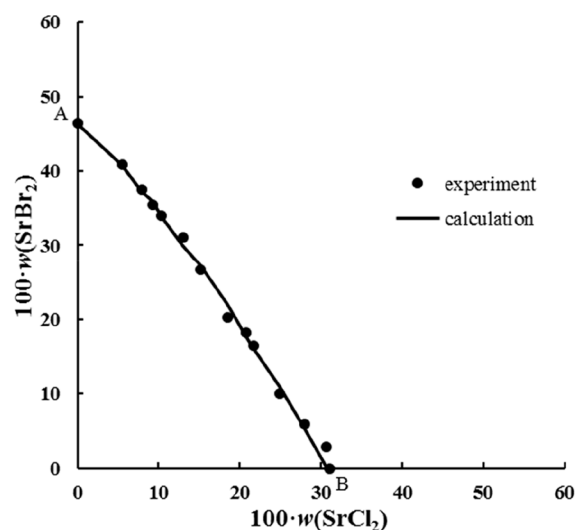
Figure 9. Experimental and calculated solubilities in the ternary system $SrCl_2$–$SrBr_2$–H_2O at 273 K: ●, experimental solubility point; tie line, calculated solubility line.

respectively. The results indicate that the changes in the trend of mean activity coefficients ($\gamma_\pm$) of $SrCl_2$ or $SrBr_2$ with its molality are approximately the same at three temperatures $T = 273$, 298, and 323 K. The trend of each curve at the three temperatures
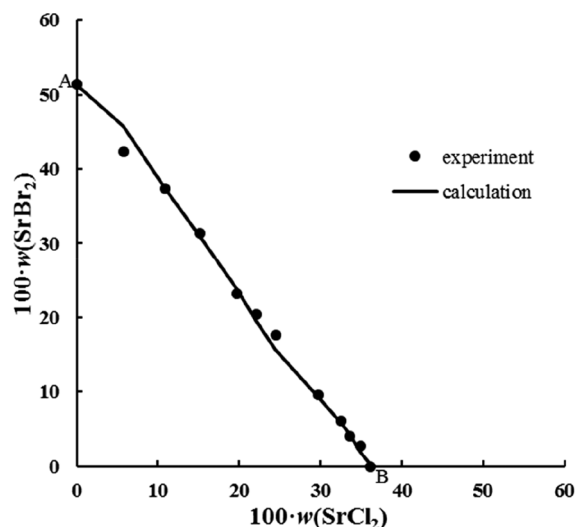
Figure 10. Experimental and calculated solubilities in the ternary system $SrCl_2-SrBr_2-H_2O$ at 298 K: ●, experimental solubility point; tie line, calculated solubility line.

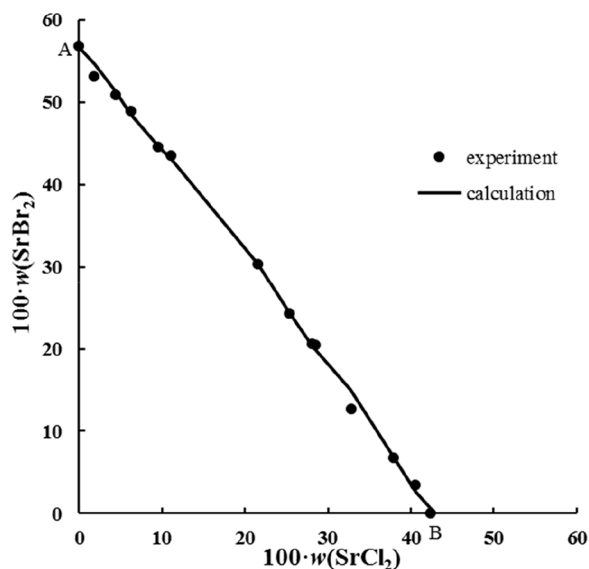**Figure 11.** Experimental and calculated solubilities in the ternary system $SrCl_2-SrBr_2-H_2O$ at 323 K: ●, experimental solubility point; tie line, calculated solubility line.

Figure 12. Mean activity coefficient ($\gamma_\pm$) of $SrCl_2$ versus liquid phase composition (m) of $SrCl_2$ at 273, 298, and 323 K.

Figure 13. Mean activity coefficient ($\gamma_\pm$) of $SrBr_2$ versus liquid phase composition (m) of $SrBr_2$ at 273, 298, and 323 K.

shows that the average activity coefficient ($\gamma_\pm$) of $SrCl_2$ increases rapidly and then decreases with the increase of its molality and that for $SrBr_2$ it increases with the increase of its molality. Obviously, the mean activity coefficients in the system at 323 K are larger than those at 298 and 273 K in Figures 12 and 13. It further illustrates the regular change in the average activity coefficient and temperature, showing a positive correlation under the same concentration conditions. Christov compared the predicted mean activity coefficients of NaCl, NaBr, KCl, KBr, $MgCl_2$, $MgBr_2$, $CaCl_2$, and $CaBr_2$ against molality (up to saturation molality) in their binary solutions at T = 298.15 K for evaluating ion interaction parameters. The results showed that the average activity coefficients of chloride or bromide of magnesium and calcium are much larger than those of chloride or bromide for sodium and potassium and can reach tens to hundreds at the saturation molality.[39] The calculated mean activity coefficients of $MgBr_2$ and $MgSO_4$ against molality in the
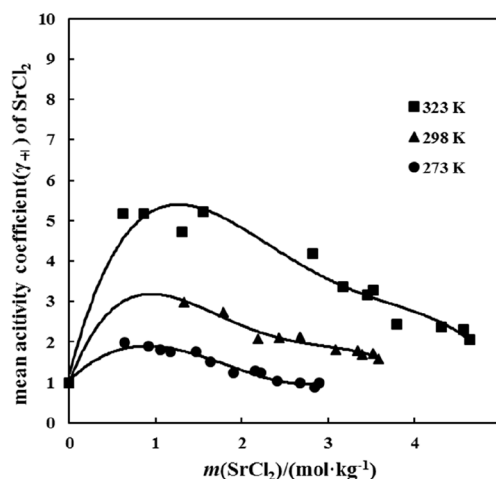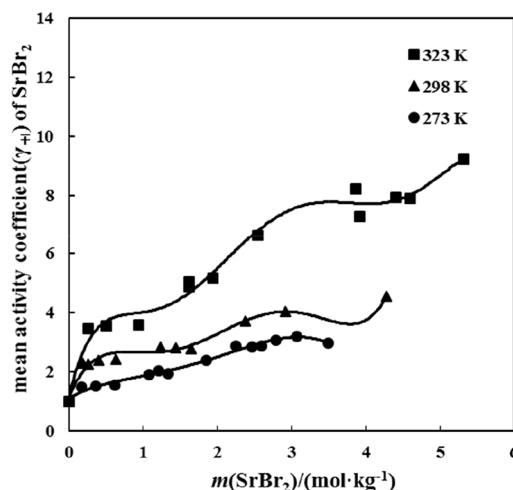
ternary solutions up to the saturation molality at 323.15 K have been discussed by Meng et al., which indicated that mean activity coefficients of $MgBr_2$ and $MgSO_4$ have large values owing to their highly soluble properties.[40]

4. CONCLUSIONS

Measurements of mineral solubilities in the ternary system $SrCl_2-SrBr_2-H_2O$ were carried out at 273, 298, and 323 K and 0.1 MPa using an isothermal dissolution equilibrium method. According to the experimental solubility data, the phase diagrams of the system at 273, 298, and 323 K were plotted. The results show that the phase diagrams at three temperatures for the ternary system $SrCl_2-SrBr_2-H_2O$ belong to the complete solid solution type, rather than double salt or simple cosaturated type. And in the ternary system $SrCl_2-SrBr_2-H_2O$, no invariant point, an univariant curve, and a crystallization region corresponding to solid solution $Sr(Cl, Br)_2\cdot6H_2O$ participate in constructing the solid-liquid equilibrium phase diagrams at 273, 298, and 323 K. On the basis of Pitzer electrolyte solution theoretical model, the calculated solubility diagrams were constructed, which were basically consistent with the experimental measurements. The results are of great use for

surmounting the intractable problem of strontium enrichment in comprehensive utilization of brine.

■ AUTHOR INFORMATION

Corresponding Author

Shi-Hua Sang − *College of Material and Chemistry & Chemical Engineering, Chengdu University of Technology, Chengdu 610059, People's Republic of China;* ⊙ orcid.org/0000-0002-5948-3882; Phone: 13032845233; Email: sangshihua@sina.com.cn

Authors

Xue-Ping Zhang − *College of Material and Chemistry & Chemical Engineering, Chengdu University of Technology, Chengdu 610059, People's Republic of China; College of Chemistry & Chemical Engineering, Sichuan University of Arts & Science, Dazhou 635000, People's Republic of China*

Han-Zhong Zhang − *College of Material and Chemistry & Chemical Engineering, Chengdu University of Technology, Chengdu 610059, People's Republic of China*

Lan-Rong Zhao − *College of Material and Chemistry & Chemical Engineering, Chengdu University of Technology, Chengdu 610059, People's Republic of China*

Complete contact information is available at:
https://pubs.acs.org/10.1021/acs.jced.0c00478

Notes

The authors declare no competing financial interest.

■ REFERENCES

(1) Gogda, A. A.; Patidar, R.; Rebary, B. Geological introduction to strontium-rich sub-soil brine with emphasis on the Little Rann of Kutch and Bhavnagar, Gujarat. *J. Geol. Soc. India* **2017**, *89*, 82−86.

(2) Assarsson, G. O.; Balder, A. Equilibria between 18°C and 100°C in the aqueous systems containing Sr^{2+}, Mg^{2+} and Cl^-. *J. Phys. Chem.* **1954**, *58*, 416−418.

(3) Assarsson, G. O.; Balder, A. Equilibria between 18° and 114° in the aqueous ternary system containing Ca^{2+}, Sr^{2+}, and Cl^-. *J. Phys. Chem.* **1953**, *57*, 717−722.

(4) Assarsson, G. O. Equilibria in aqueous systems containing Sr^{2+}, K^+, Na^+ and Cl^-. *J. Phys. Chem.* **1953**, *57*, 207−210.

(5) Li, D. W.; Sang, S. H.; Cui, R. Z.; Wei, C. Solid−liquid equilibria in the ternary systems $NaCl-SrCl_2$ − H_2O and $KCl-SrCl_2-H_2O$ at 348 K. *J. Chem. Eng. Data* **2015**, *60*, 1227−1232.

(6) Liu, Q.; Gao, Y. Y.; Zhang, W. Y.; Sang, S. H. Solid-liquid equilibria in ternary system $SrBr_2-MgBr_2-H_2O$ at (298 and 323) K. *J. Chem. Eng. Jpn.* **2018**, *51*, 1−5.

(7) Li, D.; Meng, L. Z.; Deng, T. L.; Guo, Y. F.; Pan, Yu Experimental and thermodynamic modeling study of solid-liquid equilibrium in ternary systems $NaBr-SrBr_2-H_2O$ and $KBr-SrBr_2-H_2O$ at 288.15 K and 0.1 MPa. *J. Mol. Liq.* **2018**, *252*, 362−367.

(8) Ye, C.; Gao, Y. Y.; Sang, S. H.; Jiang, P. H.; Ge, Q. Studies on phase equilibria in the ternary $KBr-SrBr_2-H_2O$ and $NaBr-SrBr_2-H_2O$ systems at 308 K. *J. Chem. Eng. Jpn.* **2020**, *53*, 183−189.

(9) Cui, R. Z.; Nie, G. L.; Sang, S. H.; Yang, L.; Wang, Z. C. Measurements of (solid+liquid) phase equilibria in the quaternary system $NaBr + KBr + SrBr_2 + H_2O$ and two subsystems $NaBr+SrBr_2+H_2O$ and $KBr + SrBr_2 + H_2O$ at $T = 323$ K. *J. Chem. Eng. Data* **2017**, *62*, 3187−3192.

(10) Hu, J. X.; Sang, S. H.; Zhang, T. T.; Cui, R. Z.; Wang, D.; Zhang, X. P. Solid−liquid equilibria in the systems $CaBr_2-MgBr_2-H_2O$ and $NaBr-KBr-SrBr_2$ at 348 K. *J. Chem. Eng. Data* **2015**, *60*, 3087−3092.

(11) Niu, Z. D.; Cheng, F. Q.; Li, B. C.; Cheng, X. *Water salt system phase diagram and its application* (in Chinese); Tianjin University Press: Tianjing, China, 2002.

(12) Li, D.; Meng, L. Z.; Deng, T. L.; Guo, Y. F.; Fu, Q. T. Thermodynamic study of solid−liquid equilibrium in $NaCl-NaBr-H_2O$ system at 288.15 K. *J. Russ. Phys. Chem. A* **2018**, *92*, 1213−1218.

(13) Weng, Y. B.; Wang, J. K.; Ying, Q. X.; Wang, Y. F. Solid-liquid equilibrium of $NaCl-NaBr-H_2O$ ternary system (in Chinese). *Petrochem. Tech.* **2007**, *36*, 358−361.

(14) Sang, S. H.; Cui, R. Z.; Hu, Y. X.; Zeng, X. X. Measurements and calculations of solid-liquid equilibria in the ternary system $NaCl-NaBr-H_2O$ at 323 K. *J. Solution Chem.* **2014**, *43*, 2133−2143.

(15) Sang, S. H.; Hu, Y. X.; Cui, R. Z.; Hu, J. X.; Wang, Y. Measurements of solid-liquid equilibria in the ternary system $NaCl-NaBr-H_2O$ at 373 K. *J. Russ. Phys. Chem. A* **2015**, *89*, 1152−1157.

(16) Meng, L. Z.; Li, D.; Ma, C. Y.; Liu, K. X. Measurement and thermodynamic model study on equilibrium solubility in the ternary system $KCl-KBr-H_2O$ at 323.15 K. *J. Russ. Phys. Chem. A* **2014**, *88*, 2283−2288.

(17) Hu, Y. X.; Sang, S. H.; Cui, R. Z.; Zhong, S. Y. Solid−liquid equilibria in the ternary system $KCl-KBr-H_2O$ at 348 K. *J. Chem. Eng. Data* **2014**, *59*, 802−806.

(18) Meng, L. Z.; Li, D.; Deng, T. L.; Guo, Y. F.; Ma, R. Measurement and thermodynamic model study on equilibrium solubility in the aqueous system of magnesium chloride and magnesium bromide. *CALPHAD: Comput. Coupling Phase Diagrams Thermochem.* **2013**, *43*, 105−111.

(19) Qiu, D.; Ren, B. S. Phase equilibrium study of system $MgCl_2-MgBr_2-H_2O$ at 25°C. *J. Heibei Univ. Technol.* **2002**, *31*, 32−35.

(20) Li, D.; Li, S. S.; Meng, L. Z.; Deng, T. L.; Guo, Y. F. Solid−liquid phase equilibria of ternary systems $LiCl-LiBr-H_2O$ and $CaCl_2-CaBr_2-H_2O$ at 288.15 K. *J. Chem. Eng. Data* **2017**, *62*, 833−838.

(21) Fosbøl, P. L.; Thomsen, K.; Stenby, E. H. Reverse Schreine-makers method for experimental analysis of mixed-solvent electrolyte systems[J]. *J. Solution Chem.* **2009**, *38*, 1−14.

(22) Yao, Y.; Cai, R. H.; Gao, S. B.; Wang, G. Q.; Zhang, H. F.; Zhang, Y. S. Improvement of the determination method for bromide ion in seawater and brine (in Chinese). *Salt Ind. Chem. Ind.* **2012**, *41*, 24−27.

(23) Haynes, W. M., Ed. *CRC Handbook of Chemistry and Physics*, 97th ed.; CRC Press: Boca Raton, FL, USA, 2016.

(24) Harvie, C. E.; Weare, J. H. The prediction of mineral solubilities in natural waters: the $Na-K-Mg-Ca-Cl-SO_4-H_2O$ system from zero to high concentration 25°C. *Geochim. Cosmochim. Acta* **1980**, *44*, 981−997.

(25) Harvie, C. E.; Eugster, H. P.; Weare, J. H. Mineral equilibria in the six-component seawater system, $Na-K-Mg-Ca-SO_4-Cl-H_2O$ at 25°C. II: compositions of the saturated solutions. *Geochim. Cosmochim. Acta* **1982**, *46*, 1603−1618.

(26) Harvie, C. E.; Møller, N.; Weare, J. H. The prediction of mineral solubilities in natural waters: the $Na-K-Mg-Ca-H-Cl-SO_4-OH-HCO_3-CO_3-CO_2-H_2O$ system from zero to high ionic strengths at 25°C. *Geochim. Cosmochim. Acta* **1984**, *48*, 723−751.

(27) Balarew, C.; Christov, C.; Petrenko, S.; Valyashko, V. Thermodynamics of formation of carnallite type double salts. *J. Solution Chem.* **1993**, *22*, 173−181.

(28) Christov, C. Thermodynamics of the aqueous sodium and magnesium bromide system at the temperatures 273.15 and 298.15 K. *CALPHAD: Comput. Coupling Phase Diagrams Thermochem.* **1996**, *20*, 501−509.

(29) Spencer, R. J.; Møller, N.; Weare, J. H. The prediction of mineral solubilities in natural water: a chemical equilibrium model for the $Na-K-Ca-Mg-Cl-SO_4-H_2O$ system at temperature below 298.15 K. *Geochim. Cosmochim. Acta* **1990**, *54*, 575−590.

(30) Phutela, R. C.; Pitzer, K. S.; Saluja, P. P. S. Thermodynamics of aqueous magnesium chloride, calcium chloride, and strontium chloride at elevated temperatures. *J. Chem. Eng. Data* **1987**, *32*, 76−80.

(31) Roy, R. N.; Roy, L. N.; Ingle, A. L.; Davis, W. B.; Larkin, D. W.; Johnson, D. A.; Hnath, E. J.; Millero, F. J. The study of activity coefficients of (hydrogen bromide+strontium bromide)(aq) using Pitzer's formalism. *J. Chem. Thermodyn.* **1992**, *24*, 425−438.

(32) Goldberg, R. N.; Nuttall, R. L. Evaluated activity and osmotic coefficients for aqueous solutions: the alkaline earth metal halides. *J. Phys. Chem. Ref. Data* **1978**, *7*, 263−310.

(33) Patil, K. R.; Tripathi, A. D.; Pathak, G.; Katti, S. S. Thermodynamic properties of aqueous electrolyte solutions. 2. Vapor pressure of aqueous solutions of sodium bromide, sodium iodide, potassium chloride, potassium bromide, potassium iodide, rubidium chloride, cesium chloride, cesium bromide, cesium iodide, magnesium chloride, calcium chloride, calcium bromide, calcium iodide, strontium chloride, strontium bromide, strontium iodide, barium chloride, and barium bromide. *J. Chem. Eng. Data* **1991**, *36*, 225−230.

(34) Salamat-Ahangari, R. Isopiestic investigation of the ternary system NaBr+NaCl+H_2O at 298.15 K. *J. Mol. Liq.* **2016**, *219*, 1000−1005.

(35) Hribar, B.; Southall, N. T.; Vlachy, V.; Dill, K. A. How ions affect the structure of water. *J. Am. Chem. Soc.* **2002**, *124*, 12302−12311.

(36) Fan, C. M.; Shu, L.; Yu, H. R.; Shi, Y. F. Calculation of the solubility data of the K_2SO_4−$(NH_4)_2SO_4$−H_2O and KCl−NH_4Cl−H_2O three-component systems containing solid solution. *J. Chem. Eng. Chin. Univ.* **1998**, *12*, 64−69.

(37) Weng, Y. B.; Wang, Y. F.; Wang, J. K.; Yin, Q. X. Phase diagram for the ternary system of K^+/Cl^-, Br^-−H_2O at 298 K, 313 and 333 K. *J. Chem. Eng. Chin. Univ.* **2007**, *21*, 695−699.

(38) Steiger, M. Thermodynamic properties of $SrCl_2$ (aq) from 252 to 524 K and phase equilibria in the $SrCl_2$−H_2O system: Implications for thermochemical heat storage. *J. Chem. Thermodyn.* **2018**, *120*, 106−115.

(39) Christov, C. Study of bromide salts solubility in the (m_1KBr+m_2CaBr$_2$)(aq) system at T = 323.15K. Thermodynamic model of solution behavior and (solid+liquid) equilibria in the ternaries (m_1KBr+m_2CaBr$_2$)(aq), and (m_1MgBr$_2$+m_2CaBr$_2$)(aq), and in the quinary (Na+K+Mg+Ca+Br+H_2O) systems to high concentration and temperature. *J. Chem. Thermodyn.* **2012**, *55*, 7−22.

(40) Meng, L. Z.; Deng, T. L.; Guo, Y. F.; Li, D.; Yang, L. Measurement and thermodynamic model study on solid+liquid equilibria and physicochemical properties of the ternary system MgBr$_2$+ MgSO$_4$+H_2O at 323.15 K. *Fluid Phase Equilib.* **2013**, *342*, 88−94.